European Journal of Pharmaceutical Sciences 48 (2013) 55–63

Contents lists available at SciVerse ScienceDirect

European Journal of Pharmaceutical Sciences

journal homepage: www.elsevier.com/locate/ejps

Cell-surface glycosaminoglycans inhibit intranuclear uptake but promote post-nuclear processes of polyamidoamine dendrimer–pDNA transfection

Zarrintaj Ziraksaz [a,b,1], Alireza Nomani [c,*,1], Marika Ruponen [d], Masoud Soleimani [b,e], Majid Tabbakhian [a], Ismaeil Haririan [f]

[a] Department of Pharmaceutics and Isfahan Pharmaceutical Sciences Research Center, School of Pharmacy and Pharmaceutical Sciences, Isfahan University of Medical Sciences, Isfahan, Iran
[b] Department of Molecular Biology and Genetic Engineering, Stem Cell Technology Research Center, 15856 36473 Tehran, Iran
[c] Department of Pharmaceutics, School of Pharmacy, Zanjan University of Medical Sciences, P.O. Box 56184 45139, Zanjan, Iran
[d] School of Pharmacy, Faculty of Health Sciences, University of Eastern Finland, Kuopio, Finland
[e] Hematology Department, School of Medical Sciences, Tarbiat Modares University, Tehran, Iran
[f] Department of Pharmaceutics, School of Pharmacy, Tehran University of Medical Sciences, Tehran, Iran

ARTICLE INFO

Article history:
Received 13 February 2012
Received in revised form 31 August 2012
Accepted 18 October 2012
Available online 3 November 2012

Keywords:
Glycosaminoglycan
Polyamidoamine dendrimer
Transfection
Intranuclear kinetics
Intracellular kinetics
Heparan sulphate proteoglycan

ABSTRACT

Background: Interaction of cell-surface glycosaminoglycans (GAGs) with non-viral vectors seems to be an important factor which modifies the intracellular destination of the gene complexes. Intracellular kinetics of polyamidoamine (PAMAM) dendrimer as a non-viral vector in cellular uptake, intranuclear delivery and transgene expression of plasmid DNA with regard to the cell-surface GAGs has not been investigated until now.

Methods: The physicochemical properties of the PAMAM–pDNA complexes were characterized by photon correlation spectroscopy, atomic force microscopy, zeta measurement and agarose gel electrophoresis. The transfection efficiency and toxicity of the complexes at different nitrogen to phosphate (N:P) ratios were determined using various in vitro cell models such as human embryonic kidney cells, chinese hamster ovary cells and its mutants lacking cell-surface GAGs or heparan sulphate proteoglycans (HSPGs). Cellular uptake, nuclear uptake and transfection efficiency of the complexes were determined using flow cytometry and optimized cell-nuclei isolation with quantitative real-time PCR and luciferase assay.

Results: Physicochemical studies showed that PAMAM dendrimer binds pDNA efficiently, forms small complexes with high positive zeta potential and transfects cells properly at N:P ratios around 5 and higher. The cytotoxicity could be a problem at N:Ps higher than 10. GAGs elimination caused nearly one order of magnitude higher pDNA nuclear uptake and more than 2.6-fold higher transfection efficiency than CHO parent cells. However, neither AUC of nuclear uptake, nor AUC of transfection affected significantly by only cell-surface HSPGs elimination and interesting data related to the effect of GAGs on intranuclear pDNA using PAMAM as delivery vector have been reported in this study.

Conclusion: Presented data shows that the rate-limiting step of PAMAM–pDNA complexes transfection is located after delivery to the cell nucleus and GAGs are regarded as an inhibitor of the intranuclear delivery step, while slightly promotes transgene expression.

1. Introduction

Successful gene therapy is still lacking an ideal vector which is safe and efficient in delivering genes to the nucleus of the target cells in vivo (Boulaiz et al., 2005). Viral vectors enable high transgene expression but their clinical usage is limited due to the concerns related to safety profile and large scale production. Non-viral vectors, on the other hand, are relatively safe and easier to produce but their low gene delivery efficiency is the main bottleneck. Understanding of the detailed mechanisms and the main barriers in gene delivery both at extra- and intracellular levels and post-nuclear processes including transcription and translation of the transgene offers new perspective of the previously used vectors and designing of new proper vectors.

After reaching the cell surface, positively charged non-viral gene delivery systems bound to negatively charged cell membrane. The main molecules responsible for surface charge of the cell membrane are glycosaminoglycans (GAGs) which encompass the

* Corresponding author. Tel./fax: +98 241 4273639.
E-mail address: arnomani@zums.ac.ir (A. Nomani).
[1] These two authors contributed equally to this article.

0928-0987/$ - see front matter © 2012 Elsevier B.V. All rights reserved.
http://dx.doi.org/10.1016/j.ejps.2012.10.016

whole cell surface of all mammalian cells (Ruoslahti, 1988). GAGs have important roles in cell adhesion, differentiation, proliferation and growth (Ruoslahti, 1988), and they are known for acting as primary receptors for numerous viral particles (Liu and Thorp, 2002; Tuve et al., 2008). In non-viral gene delivery the exact role of GAGs is contradictory. Some studies have shown that GAGs promote delivery and transfection of non-viral vectors (Mislick and Baldeschwieler, 1996; Mounkes et al., 1998; Payne et al., 2007). However, there are also studies suggesting that cell-surface GAGs act as receptors for non-viral gene delivery complexes but have inhibitory effect on transgene expression (Belting and Petersson, 1999; Lampela et al., 2004; Ruponen et al., 2004). This indicates that cell-surface GAGs may define the intracellular fate of the complexes but their exact role in intracellular steps is still poorly understood.

Tomalia et al. (1984) were the first group to introduce polyamidoamine (PAMAM) dendrimers as potential gene delivery carriers. PAMAM dendrimers are hyper-branched, symmetrical and monodisperse polymeric molecules consisting of three parts i.e. core, branches and surface groups in molecular structure. The step by step synthesis of a dendrimeric structure results in the final product with very uniform structure and size at each generation. Due to the surface primary amino groups PAMAM dendrimers are extremely positively charged and thus able to interact with DNA and form stable gene delivery complexes. Various generations of PAMAM dendrimers have been evaluated for gene delivery (Bielinska et al., 1999; Haensler and Szoka, 1993; Kukowska-Latallo et al., 1996; Mitra and Imae, 2004; Su et al., 2009). Haensler and Szoka (1993)) showed that higher generations of PAMAM (generations with diameter higher than 6.8 nm) are efficient transfection agents. One explanation for high transfection efficiency is the buffering capacity of the PAMAM dendrimer which facilitates proton sponge effect (Yang and May, 2008) and triggers escape of the complexes from the endosomes to the cytosol. Unfortunately, higher generations of PAMAM dendrimer (generations 6 and above) possess high toxicity which limits their usage. Strategies trying to overcome toxicities have been proposed (Huang et al., 2007; Tang et al., 1996; Wang et al., 2009). Since the molecular surface amine density is supposed to be the main reason for the cytotoxicity of PAMAM dendrimers, most of these strategies have focused on reducing this surface amine density by PEGylation (Wang et al., 2009), fracturing some of the internal branches (Tang et al., 1996) and acetylation (Kolhatkar et al., 2007). One option to reduce cytotoxicity is to use lower generations of dendrimers, despite of their lower transfection efficiency.

Recently, we have shown that the generation five of PAMAM dendrimer (which is regarded as a lower generation of PAMAM) can act as a suitable carrier for antisense oligonucleotide. We showed that the dendrimer was able to compact and deliver antisense efficiently to the breast cancer cells (Nomani et al., 2010). To our knowledge, PAMAM has not been evaluated yet to obtain its intracellular, intranuclear and transfection kinetics as a gene delivery vector.

In this study, we applied generation five of PAMAM dendrimer for delivery of pDNA. Firstly, the physicochemical properties of PAMAM–pDNA complexes in terms of size, charge, morphology and stability was evaluated using photon correlation spectroscopy (PCS), atomic force microscopy (AFM) and gel electrophoresis (GE). Secondly, the cell uptake and transfection efficiency of the PAMAM–pDNA complexes were clarified by fluorescent microscopy and flow cytometry and then the cytotoxicity was determined by MTT test. Finally, the role of cell-surface GAGs on the intracellular kinetics of PAMAM–pDNA complexes both at intranuclear and post-nuclear level were investigated using optimized cell-nuclei isolation and real-time PCR methods. We have shown that PAMAM dendrimer at generation five is a promising agent for pDNA delivery. However, the rate limiting step of PAMAM mediated gene delivery seems to be at the post-delivery steps including transcription and/or translation processes. Altogether, the obtained data confirm that cell-surface GAGs have subtle effects on the cell uptake and intracellular kinetics of PAMAM–pDNA complexes.

2. Materials and methods

2.1. Cell cultures

CHO (Chinese hamster ovary) cells were a kind gift from Dr. Seppo Yla-Herttuala (University of Eastern Finland, Finland). CHO cells were maintained in Dulbecco's modified Eagle's medium (DMEM; Gibco) supplemented with 10% (v/v) foetal bovine serum (FBS; Gibco), 2 mM L-glutamine (EuroClone) and 100 units/ml penicillin- streptomycin (PEST; EuroClone S.p.A.). PgsB-618 and pgsD-677 cell lines are CHO mutant cells which were purchased from ATCC. PgsB-618 cells are devoid of galactosyltransferase I activity and thus are not able to produce any proteoglycans (called glycosaminoglycans- or GAGs-deficient cells). These cells were grown in medium containing Ham's F12 (GIBCO), 10% (v/v) FBS, 2 mM L-glutamine and 100 units/ml PEST. PgsD-677 cells are lacking heparan sulphate polymerase activity which is required for heparan sulphate synthesis (called heparan sulphate proteoglycans- or HSPG-deficient cells). This cell line was maintained in F12K Nutrient Mixture, Kaighn's (GIBCO) complemented with 10% FBS, and PEST (100 units/ml). HEK-293T (Human embryonic kidney) cell line (HEK), were purchased from National Cell Bank of Iran, Pasteur Institute (passage number between 15 and 40) and were grown in DMEM medium supplemented with 10% heat-inactivated FBS and PEST. All cell lines were grown at 37 °C in 7% CO_2 and were subcultured 2–3 times a week.

2.2. Plasmids

The CMV-driven luciferase reporter plasmid (pCLuc4 or pLuc) was donated by Dr. F.C. Szoka, Jr. (UCSF, San Francisco, USA) and plasmid expressing enhanced green fluorescent protein (pEGFP-C1 or pEGFP) was purchased from Invitrogen Co. (Carlsbad, USA). The plasmids were amplified in *E. Coli* and purified in an ion-exchange column (Qiagen, Hilden, Germany) according to the manufacturer's instructions. The purity and the concentration of the plasmid were determined by absorbance at 260 nm and 280 nm. The integrity of plasmid was confirmed by agarose gel electrophoresis.

2.3. Dendrimer synthesis

Amine terminated generation 5 polyamidoamine dendrimer (PAMAM) was synthesized and characterized according to the method described earlier (Nomani et al., 2010). Briefly, the synthesis was performed via iterative reactions of Michael addition of methylacrylate to the ethylenediamine for half generations followed by exhaustive amidation of half generations by high excess methanolic ethylenediamine at the next step for full generations. The product at each step was purified by ultrafilteration (MWCO of 3000 Da) followed by the freeze drying. The final product was characterized by ^{1}HNMR, FT-IR and gel permeation chromatography.

2.4. Formation of the gene delivery complexes

Complexes composed of PAMAM–pEGFP were formed in double-distilled water (ddH_2O) at primary amines of dendrimer to phosphate groups of plasmid (N:P) ratios of 0.5, 1, 2.5, 5, 10 and

20. First, plasmid stock solution was diluted in ddH_2O to obtain a 40 μg/ml concentration. The dendrimer solutions of various concentrations were prepared by diluting the dendrimer stock solution with ddH_2O. The dendrimer solution (100 μl) was then added to an equal volume of plasmid solution so as to obtain the desired N:P ratios. After proper mixing, the gene delivery complexes were incubated for 10–15 min at room temperature. Complexes containing PAMAM and pCLuc4 plasmid (PAMAM-pLuc) were always prepared at N:P ratio of 4.

Commercially available Lipofectamine™ 2000 (Invitrogen Co., Carlsbad, USA) gene delivery complexes were prepared according to the manufacturer's instruction.

2.5. Particle size and zeta potential analysis

The concentration of the gene delivery complexes, which were prepared as described earlier, was 0.5 μg/ml. The size or zeta potential of the complexes was evaluated immediately after preparation using Malvern Nanosizer ZN series according to the manufacturer's instructions (Malvern Instruments Ltd., Worcestershire, UK). The particle size analysis was based on the intensity values and the disposable capillary cells (catalogue number: DTS1061) were used for size and zeta potential measurements of each sample at the same time.

2.6. Agarose gel electrophoresis

Gel electrophoresis experiments were performed using 1% w/v agarose gel in a 1 M Tris–acetate–EDTA (TAE) buffer solution. PAMAM–pEGFP complexes were formed at different charge ratios as described above. Complexes containing 1 μg of pDNA mixed with 4 μl of loading dye were loaded onto gel. Amount of 1 μg of free pDNA was used as control. The samples were run for 45 min at 110 V. Then, the gel was incubated in 0.5% ethidium bromide solution for 20 min and visualized under UV illumination by UV documentation device.

2.7. Atomic force microscopy (AFM) analysis of the complexes

For AFM experiments, PAMAM–pEGFP complexes were formed at N:P ratios of 0.5, 1, 2.5, 5, 10 and 20 similar to the particles size analysis experiments. The prepared complexes were diluted 100 folds and 5 μl of each formulation was dropped on a freshly cleaved mica sheet, dried at room temperature and washed twice by ddH_2O (100 μl). After exposing complexes to a gentle air flow for 10 min, the analysis was performed using a DME DualScope/Rasterscope™ SPM (DME Co., Denmark). The AFM studies were performed at AC mode, spring constant of 2.8 N/m with resonance frequency of 100 kHz, speed of 30–40 μm/s, and force constant of 42 N. The processing of topographic or phase images was carried out using DME SPM software version 2.1.1.2 (DME Co., Denmark).

2.8. Fluorescence microscopy and flow cytometry

GFP transgene expression was visualized by fluorescence microscopy for HEK, CHO or its mentioned mutant cells and then quantified by flow cytometry method (performed only for CHO cells). For these studies, HEK, CHO parent or mutant cells were seeded in a 6-well plate (3×10^5 cells/well) one day before transfection. The PAMAM–pDNA complexes at different N:P ratios (0.5, 1, 2.5, 5, 10 and 20) and Lipofectamine™ complexes were prepared as described earlier. The cells were exposed to the complexes for 4 h using the FBS-free cell culture medium. After exposure, the cells were washed and fresh FBS-containing medium was added to the cells. After 48 h incubation, the medium was removed and the cells were washed with phosphate buffered saline solution. After that, for fluorescent microscopy, green fluorescent protein expression of the cells was evaluated by inverted fluorescent microscopy (Olympus I×50, Olympus Inc.) at 200× and 400× magnifications. In the case of flow cytometry analysis, the transfected cells were firstly detached from culture plates by trypsin–EDTA and washed twice with PBS. Then GFP expression was quantified by flow cytometry (Partec GmbH, Münster, Germany) using 532 nm green Nd:YAG laser light source and Side scatter vs. FL1 plot. In order to eliminate the autofluorescence of the cells, appropriate gating was set up using untransfected cells. For each sample 10,000 gated events were collected. The presented results are averages of at least two replicates.

2.9. Cellular uptake

For cellular uptake studies parent or mutant CHO cells were transfected with PAMAM-pLuc at N:P ratio of 4 and Lipofectamine™-pLuc as described earlier for pEGFP. The cells were exposed to complexes at +4 or +37 °C for 4 h. After incubation, the cells were washed by PBS and lyzed by distilled water, while the culture plates were kept on ice. Afterward, the amount of uptaken pDNA was evaluated using qRT-PCR by subtracting the values obtained at +4 °C from the values obtained at +37 °C.

2.10. Cell viability

The effect of the prepared Lipofectamine™- or PAMAM–pDNA complexes on the cell viability was tested by 3-(4,5-dimethythiazol-2-yl)-2,5-diphenyl tetrazolium bromide (MTT) assay. One day before transfection, HEK or CHO parent cells were seeded onto 96-well culture plates (10,000 cells/well). The complexes were prepared as for the fluorescent microscopy analysis and the N:P ratios were as 0.5, 1, 2.5, 5, 10 and 20. Volume of 200 μl of the complexes were added to each well and incubated for 4 h after which the cells were washed and fresh medium added to the cells, then incubated for further 48 h. Finally, MTT assay was performed according to the previously described method (Nomani et al., 2010).

2.11. Nuclei isolation from the cells

The nuclei were isolated from CHO, pgsB-618 and pgsD-677 cell samples after transfection by PAMAM-pLuc complexes (N:P of 4) at the time points of 0, 4, 8, 12, 16, 30 and 54 h post-transfection. The cells seeded on 150 mm dishes were transfected with total of 15 μg pDNA per dish. The isolation of the nuclei was according to the previously described method based on iodixanol gradient with some modifications (Cohen et al., 2009). Briefly, the transfected cells at each time point were detached from petri dishes (4×10^6 cells/petri dishes) by trypsinization, washed twice with PBS and divided into two equal parts for nuclei isolation and protein expression analysis. Generally, to reduce the variations in intranuclear pDNA and corresponding protein expressions, the same transfected samples were used for all time points. For nuclei isolation, first part of the washed cells were resuspended in 500 μl hypo-osmotic homogenization medium (HHM) (1 mM KCl, 10 mM MgCl2, 5 mM Hepes-NaOH, pH 7.4). This cell suspension was incubated on ice for 20 min after which the cells were passed 15 times through 25G needle using a 1 ml syringe. The disruption of the cell membrane was optimized for each cell line by visualizing Trypan blue stained cells under microscope and by measuring the release of lactate dehydrogenase (LDH) enzyme from the cells using LDH assay kit (Promega Co., USA). After disruption of the cell membrane, the samples were centrifuged (1500g, 5 min, 4 °C) and the cell pellet was resuspended in 25% iodixanol solution (OptiPrep™, Axis-Shield Co., Norway) which was diluted from 60% stock solu-

tion with a buffer solution comprising 25 mM KCl, 5 mM MgCl2, 20 mM Tricine-KOH, pH 7.8. A discontinuous iodixanol gradient was prepared in 2 ml eppendorf tube by adding 35% iodixanol (500 μl) under the layer of 30% iodixanol (500 μl). Then 25% iodixanol solution containing cell sample was layered gently on the top of the gradient. The gradient was centrifuged at 10,000*g*, at 4 °C for 20 min using fixed angle rotor centrifuge (Eppendorf centrifuge model 5415 R, Eppendorf AG, Germany). The pure nuclei fraction was collected from the boundary layer of 30/35% by piercing the wall of the tube by a needle. The amount of nuclei was counted by haemocytometer. The samples were stored at −40 °C prior to the quantitative real-time polymerase chain reaction (qRT-PCR) analysis. For qRT-PCR analysis the isolated nuclei were lyzed by 0.005% (w/v) sodium dodecyl sulphate (SDS) treatment and incubating at +50 °C for 90 min. Then samples were diluted 1:50 with water and analyzed by qRT-PCR.

2.12. qRT-PCR analysis

An optimized qRT-PCR was applied to quantify the amount of cellular uptake and intranuclear pDNA (Ruponen et al., 2009). Briefly, 5 μl of each sample was mixed with 10 μl PCR reagent mixture comprising 1 μl of forward (5′-GGC GCG TTA TTT ATC GGA GTT-3′) and 1 μl reverse (5′-TAC TGT TGA GCA ATT CAC GTT CAT T-3′) primers (Sigma, Genosys, Suffolk, UK), 0.5 μl of ddH2O and 7.5 μl SYBR Green master mix (Applied Biosystems Inc., Warrington, UK). The size of the amplicon was 73 bp. The analysis was performed by employing Prism 7500 sequence detection system (Applied Biosystems, Foster City, CA) under the following PCR conditions: holding stage at 50 °C for 2 min and 95 °C for 10 min; then 40 cycles of 95 °C for 15 s and 60 °C for 1 min. A serial dilution of 10^{-6}–10^{-8} μg/μl pLuc in ddH_2O was made to generate the standard calibration curve for each experiment individually.

2.13. Luciferase protein expression assay

The second part of the transfected cell samples at each time point (0, 4, 8, 12, 16, 30 and 54 h post-transfection) which previously obtained as described in nuclei isolation experiment, was used to quantify the amount of expressed luciferase protein using Victor 1420 luminometer (Wallac Oy., Turku, Finland) according to the previously described method (Ruponen et al., 2004). Recorded luminescence activity was normalized to the protein content of each sample by Bradford assay and bovine serum albumin (Sigma–Aldrich, Germany) as the standard (Bradford, 1976).

2.14. Kinetics modeling, AUC calculation and statistical analysis

Non-compartmental modeling with extra-vascular input regarding the plasma data was considered as the proper model for calculating the area under the time-concentration curve (AUC) using WinNonlin™ version 5.2.1 software (Pharsight Co., Mountain View, CA).

Student *t*-test or one way ANOVA were used for comparison of two or more than two means, respectively. P value < 0.05 was considered as significantly different in all cases.

3. Results

3.1. Physicochemical properties of the complexes

DNA binding studies by agarose gel electrophoresis showed that PAMAM G5 was able to bound pDNA completely already at N:P ratio 1 (Fig. 1A). At N:P ratio 0.5 major fraction of the pDNA was free which was detected as a smear on the gel.

The size and zeta potential of the PAMAM–pDNA complexes measured at different N:P ratios by Nanosizer™ and AFM are presented in Fig. 1B and C and Table 1. Increasing the complexes N:P ratio above one decreased the size of particles from around 600 nm to 200 nm and from around 200 nm to 50 nm, measured by Nanosizer and AFM, respectively. Significant difference in the size of the PAMAM–pDNA complexes measured by Nanosizer or AFM was observed. The main explanation for this is the difference in the sample preparation between these two methods. For AFM, samples were dried on the mika sheet before scanning, whereas for Nanosizer the samples were dispersed in distilled water (more explanation and examples for differences in size observed by AFM and photon correlation spectroscopy methods can be found in literatures for example (de Assis et al., 2008; Singh et al., 2011)).

The zeta potential increased from −20 mV to the higher than +20 mV as a function of increasing N:P ratio (Fig. 1B). The complexes showed higher homogeneity in their size and zeta potential at N:P ratios 5 and higher. AFM showed that the particle morphologies were rather spherical at all selected N:P ratios (Fig. 1C).

3.2. In vitro transfection efficiency and cytotoxicity of the complexes

The transfection efficiency of the pEGFP-containing Lipofectamine™ and PAMAM complexes was evaluated by measuring the expression of GFP by fluorescent microscopy and flow cytometry. In the case of HEK cells, at low N:P ratio (below 5) very low or no transgene expression equal to the naked pDNA was observed (Fig. 2A (b-d)). At higher N:P ratio the transgene expression was detectable and at N:P ratio of 20 the transfection efficiency was comparable with the commercially available Lipofectamine™ (see Fig. 2A-a for Lipofectamine™ and Fig. 2A-g for N:P ratio of 20). In the case of CHO cells, the maximum GFP expression was obtained at N:P ratio of 5. According to fluorescence microscopy and flow cytometry data the transfection efficiency of PAMAM–pDNA complexes in CHO-cells was near one order of magnitude lower than that of Lipofectamine™ (Figs. 2C and 3). The cytotoxicity of the Lipofectamine™ and PAMAM complexes at different N:P ratios was determined by MTT assay for HEK and CHO cells as shown in Fig. 2B and D, respectively. The results showed that the cell viability both in HEK and CHO cells were approximately 50% at higher N:P ratios (5–20). In HEK cells, at lower N:P ratios (0.5–2.5) the cytotoxicity was between 60% to 80% for both Lipofectamine™ and PAMAM complexes (Fig. 2B). CHO cells were more sensitive to Lipofectamine™ complexes than HEK cells (Fig. 2D) but for the PAMAM complexes the trend was rather the same. Interestingly, the cytotoxicity of the PAMAM as such or in the complexed form with pDNA was rather similar in both cell lines.

3.3. Effect of cell-surface GAGs on cellular uptake, nuclear uptake and transfection efficiency

The role of cell-surface GAGs on the cellular uptake, nuclear uptake kinetics and transfection efficiency of PAMAM- and Lipofectamine-pLuc complexes was evaluated using CHO cells and CHO cell lines mutated in GAGs synthesis. The cellular uptake of pDNA was measured at +4 or +37 °C and the samples were taken 4 h post-transfection. At the lower temperature energy-dependent endocytosis cannot occur and the complexes are only able to bind to the cell surface, whereas at the higher temperature the complexes are internalized by endocytosis. The values obtained at +37 °C contain both internalized and cell-surface bound pDNA, because the used washings are not able to clean cell surface from the complexes. In order to obtain cellular uptake efficiency the values obtained at +4 °C were subtracted from the values obtained at +37 °C (Ruponen et al., 2009).

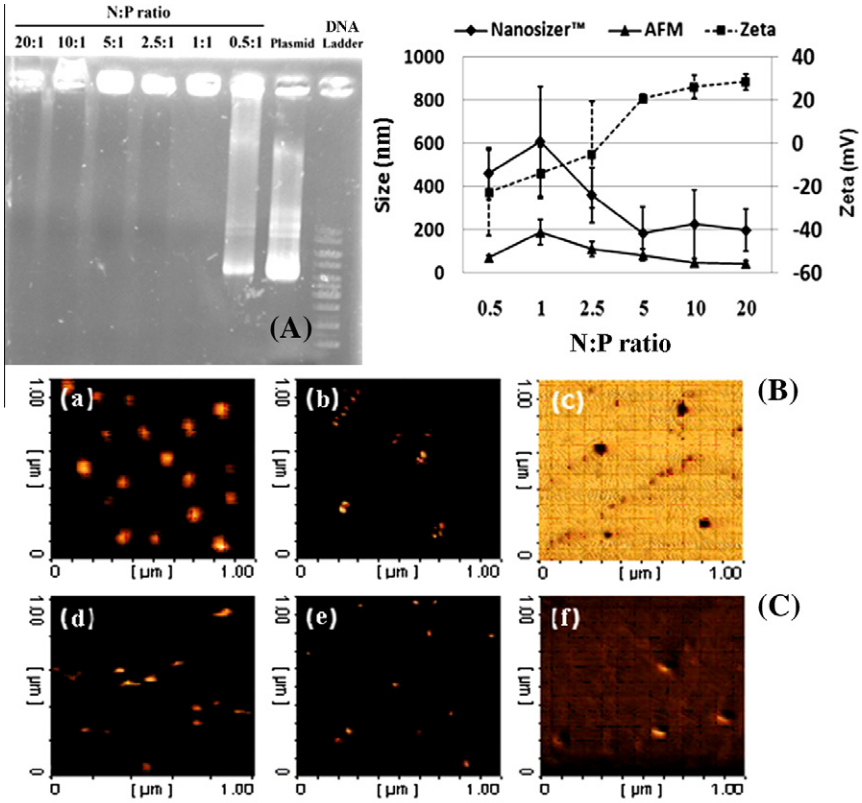

Fig. 1. (A) Agarose gel retardation analysis of PAMAM G5-pEGFP complexes carried out at various N:P ratios shown in the image. Lane plasmid corresponds to naked pDNA sample and the amount of 1 μg of pDNA is loaded in the well. (B) Size and zeta potential analysis of PAMAM-pEGFP complexes under various N:P ratios in distilled water. Particle size measured by photon correlation spectroscopy (Nanosizer™) (*closed diamond*), atomic force microscopy (*closed triangle*). The *closed squares* are zeta potential measurements. The results are shown as mean ($n = 3$) ± SD. (C) Atomic force microscopy phase or topographic images of PAMAM-pEGFP complexes formed at different N:P ratios. N:P ratios including: 0.5 (a), 1 (b), 2.5 (c), 5 (d), 10 (e) and 20 (f).

Table 1
Size distribution of PAMAM–pDNA complexes formed at different N:P ratios determined by AFM methods. For analysis, *n* particles (which is mentioned in the table) in different images were measured by the software of the device and then expressed as mean ± SD.

N:P ratio	Mean ± SD	*n*
0.5	72.15 ± 10.29	116
1	187.47 ± 58.57	87
2.5	112.68 ± 34.47	25
5	84.65 ± 27.73	72
10	49.46 ± 15.83	104
20	45.09 ± 12.11	104

Fig. 4A shows that GAGs-deficient cells had the highest cellular uptake for both PAMAM- and Lipofectamine–pDNA complexes. For PAMAM complexes, GAGs and HSPG elimination caused 9 and 4.5-fold increased cellular uptake efficiencies, respectively compared with the CHO parent cells. Showing the same trend as PAMAM, Lipofectamine™ had the highest cellular internalized pDNA for GAGs-eliminated cells. However, depending on the cell line, Lipofectamine™ revealed to be at least 8–10 folds more efficient than PAMAM in cellular uptake efficiency.

The samples for nuclear uptake of pDNA and transfection efficiency were collected at different time points (0, 4, 8, 12, 16, 30 and 54 h post-transfection) for PAMAM-pLuc complexes. The results for nuclear uptake showed that significant amount of pDNA was found inside the nucleus already 4 h after transfection (Fig. 4B). The maximum was reached around 8–16 h post-transfection. Depending on the cell line, the range of C_{max} of intranuclear pLuc was about 5×10^4 to 8.1×10^5 pLuc copies per nucleus (Fig. 4B and Table 2), after which these amounts were decreased significantly up to five folds during the next 15 h. For example, approximately 12,000 pDNA copies corresponding to about 25% of C_{max} still remained in the nucleus in CHO cells at 30 h post-transfection. Interestingly, the absence of cell-surface GAGs increased the amount of intranuclear pDNA copies by 8-fold, whereas only slight decrease was found in the absence of cell-surface HSPG (Fig. 4B and Table 2).

Transfection efficiency studies showed that at protein level the maximum was reached approximately 30 h post-transfection (Fig. 4C). The highest transfection efficiency was observed in the cells lacking GAGs. As presented in Table 2, the AUC of pgsB-618 cells was 4.51×10^8 h CPS/mg protein compared with the AUC of 1.54×10^8 and 1.74×10^8 h CPS/mg protein for pgsD-677 and CHO, respectively. This correlates relatively well with the cellular and nuclear uptake data.

Fig. 5A represents the effect of GAGs on the nuclear efficiency and Fig. 5B shows transgene expression efficiency after transfection by PAMAM. Nuclear efficiency term is obtained when nuclear uptake (AUC-values) is divided with the total initial administered dose. This value describes how efficiently administered pDNA reaches intranuclear space. Transgene expression efficiency on the other hand, defines how efficiently intranuclear pDNA is transcribed and further translated into luciferase protein. This value is calculated by dividing transfection efficiency (AUC-values) with nuclear uptake data (AUC-values). Although, it is obvious that the absence of GAGs resulted in a significantly higher efficiencies at nuclear and transfection efficiencies (see Fig. 5A for nuclear effi-

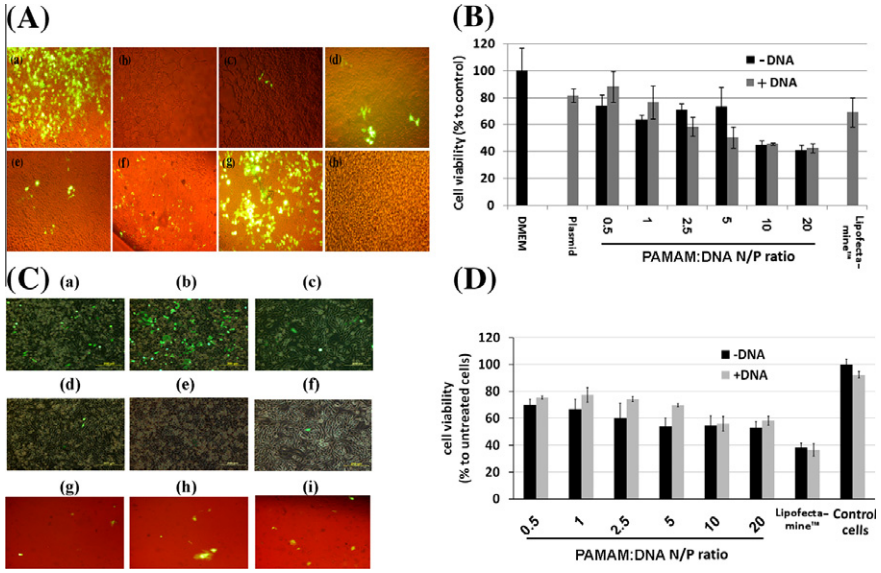

Fig. 2. (A) Fluorescent microscopy of HEK-293T cells transfected by Lipofectamine™- (a) or PAMAM G5 (b-g)-pEGFP complexes. PAMAM–pDNA complexes prepared at N:P ratios of 0.5 (b), 1 (c), 2.5 (d), 5 (e), 10 (f) and 20 (g) in comparison with the pDNA alone (h). The magnification of each image was 100–400×. The cells are shown in the background of visualized fluorescents. (B) Cell viability assay graphs (MTT test) of PAMAM-pEGFP complexes. Multiple PAMAM–pDNA N:P ratios (gray columns) were compared with their corresponding PAMAM concentration without pDNA (black columns), Lipofectamine™ at its manufacturer's recommended weight ratio, pDNA alone (plasmid) and negative control of FBS-free DMEM cell culture medium (DMEM). The data are mean ($n = 6$) relative to the negative control (DMEM or untreated) ± SEM. (C) Fluorescent microscopy evaluation of Lipofectamine™-pEGFP (a–c) for CHO, pgsB-618 and pgsD-677, respectively and PAMAM-pEGFP (d–i). PAMAM-pEGFP complexes prepared at N:P ratios of 4 in case of (d), (e) and (f), corresponding to CHO, pgsB-618 and pgsD-677 cells, respectively. The other images includes CHO at N:P ratios of 0.5 (g), 1 (h) and 5 (i). The cells are shown in the background of visualized fluorescents and 200 μm is the size of the scale bar. (D) Cell viability assay graphs (MTT test) of PAMAM-pEGFP complexes in CHO cells. Multiple PAMAM–pDNA N:P ratios (gray columns) were x compared with their corresponding PAMAM concentration without pDNA (black columns), Lipofectamine™ at its manufacturer's recommended weight ratio, pDNA alone and negative control of FBS-free CHO cell culture medium. The data are mean ($n = 6$) relative to the untreated cells ± SEM.

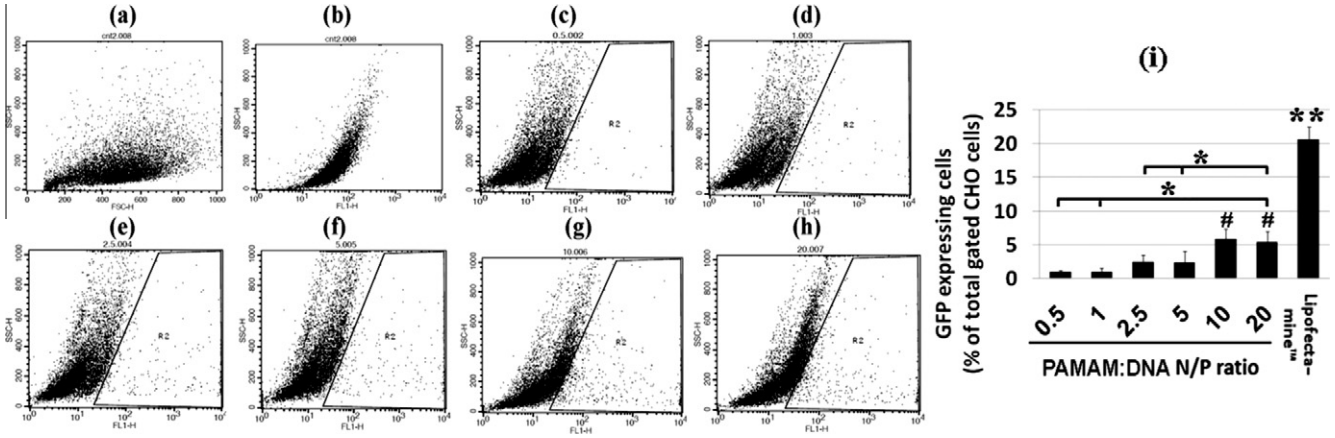

Fig. 3. Flow cytometric quantification of pEGFP expression after transfection of CHO cells using Lipofectamine™ at manufacturer's recommended weight ratio (b) and PAMAM at N:P ratios of 0.5 (c), 1 (d), 2.5 (e), 5 (f), 10 (g), and 20 (h). The images are shown as side scatter (y axis) vs. FL1 (x axis) channel corresponds to the EGFP intensity. Image (a) shows side scatter (y axis) vs. forward scatter (x axis) which is used to evaluate the cell samples qualities. Appropriate gating was performed using untransfected cells to minimize the probable autofluorescence of cells. A number of 10,000 gated events were collected for each sample and the presented results in graph (i) are mean ($n = 3$) ± S.D. $^{*}p < 0.05$, $^{**}p < 0.001$ (compared with the other treatments), # not significantly different from each other.

ciency and Fig. 4C and AUC data of protein expression in Table 2 for transfection efficiency), but a lower efficiency was detectable at transgene expression efficiency of plasmids which are successfully delivered to the nucleus (Fig. 5B). These indicate that in the absence of GAGs the administered pDNA is efficiently delivered into the nucleus, whereas the transcription/translation of the luciferase gene is less efficient in GAG-deficient cells. Moreover, Fig. 5A and B and Table 2 indicate that no clear trend could be found at neither nuclear efficiency nor transgene expression efficiency in HSPG-deficient cells compared with the CHO parent cells. Indeed, HSPG-deficient cells were as efficient as CHO parent at nuclear and transgene expression efficiencies.

4. Discussion

Polycationic dendrimers of PAMAM are regarded as a good candidate of non-viral vector and have potential to be efficient both in vitro and in vivo (Eichman et al., 2000; Navarro and Tros de ILarduya, 2009). The main goal of the present work was to shed more light on the intracellular kinetic aspect of PAMAM–pDNA complexes with emphasis on the role of cell-surface GAGs in this delivery process.

Physicochemical studies showed that PAMAM can efficiently bind to pDNA and form small complexes with a relatively high positive zeta potential (Fig. 1A to C and Table 1). PAMAM can trans-

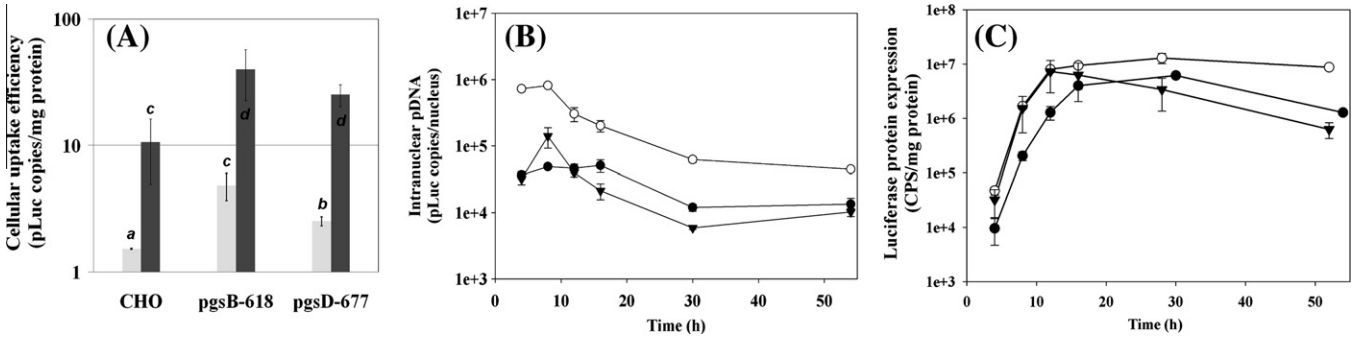

Fig. 4. (A) Quantification of cellular uptake of plasmid luciferase (pLuc) in CHO and its mutant cells transfected by PAMAM–pDNA at N:P ratio of 4 (pale gray column) and Lipofectamine–pDNA (dark gray column). The samples were incubated at 4 and 37 °C for 4 h followed by washing by PBS and detaching from culture plates. The cells were subsequently disrupted by sterile distilled water and the amount of cellular uptake of pLuc was measured by an optimized qRT-PCR. An appropriate calibration curve of pLuc in distilled water was constructed for each run of the experiment. The presented results are the subtraction of data of 4 form 37 °C and are shown as mean of three replicates ± SEM. Different letters (a–d) above the columns indicate significant difference ($p < 0.05$). (B) Comparison of nuclear uptake of pLuc in CHO parent (closed circle), pgsB-618 (open circle) and pgsD-677 (closed triangle) cells transfected by PAMAM complexes at N:P ratio of 4. The results are expressed as mean ($n = 6$) ± S.E.M. (C) Comparison of transfection efficiency after transfection of the cells by PAMAM-pLuc complexes at N:P ratio of 4 in CHO parent cells (closed circle), pgsB-618 cells (open circle) and pgsD-677 cells (closed triangle) (mean ($n = 6$) ± SEM).

Table 2
Pharmacokinetic parameters of nuclear uptake and protein expression of plasmid luciferease transfected by PAMAM–pDNA complexes in CHO parent cells, pgsB-618 cells and pgsD-677 cells. The data are calculated from the mean values of six independent samples.

Cell line	Experiment	AUC[a]	K_{el} (h^{-1})	$t_{1/2}$ (h)	C_{max}[b]	t_{max} (h)
CHO	Intranuclear pDNA	1.37E+06	0.03	23.10	5.07E+04	16
	Protein expression	1.74E+08	0.07	9.90	6.15E+03	30
pgsB-618	Intranuclear pDNA	1.09E+07	0.06	11.55	8.12E+05	8
	Protein expression	4.51E+08	0.02	34.65	1.29E+07	28
pgsD-677	Intranuclear pDNA	1.27E+06	0.13	4.91	1.40E+05	8
	Protein expression	1.54E+08	0.06	11.55	7.28E+06	12

[a] AUC of intranuclear data calculated as *h.mole of pDNA/nucleus* and for protein expression AUC is expressed as *h. luciferase count per second (CPS)/mg protein.*
[b] C_{max} of intranuclear data presented as *mole of pDNA/nucleus* and for protein expression C_{max} is expressed as *luciferase count per second (CPS)/mg protein.*

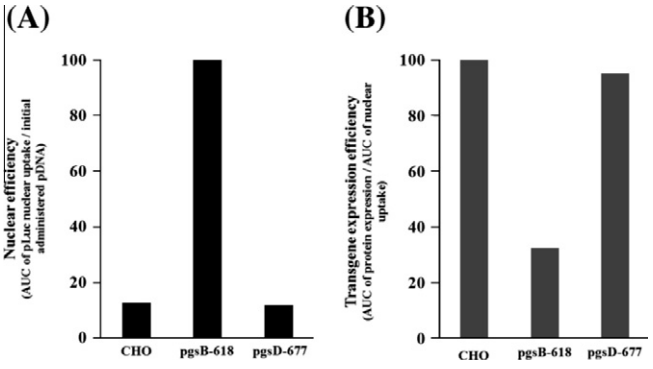

Fig. 5. Comparison of different nuclear (A) and transgene expression (B) efficiencies after transfection of parent and mutated CHO cells by PAMAM–pDNA complexes. (A) Nuclear efficiency is obtained when nuclear uptake (AUC-values) is divided with the total initial administered dose. (B) Transgene expression efficiency value is calculated by dividing the transfection efficiency (AUC-values) with the nuclear uptake efficiency (AUC-values). The AUCs are calculated from the mean values of six independent samples. The nuclear efficiency expressed as relative to the highest efficiency which was the efficiency of pgsB-618. The transgene expression efficiency expressed as relative to the efficiency of CHO cells which was the highest.

fect cells at the similar level of commercially available vector when transfecting HEK cells. In CHO cells the transfection efficiency of both used gene delivery systems was significantly lower than in HEK cells indicating that the transfection efficiency is strongly cell line dependent.

The toxicity of the polycationic vectors has been reported elsewhere (Lv et al., 2006; Nomani et al., 2010). As expected, PAMAM–pDNA complexes showed a moderate cytotoxicity compared to the Lipofectamine™. High net positive charges of the particles are regarded as a toxic factor for the cells. In general, the main mechanisms responsible for cytotoxicity of polymeric carriers of pDNA are the induction of plasma membrane and/or nuclear membrane permeability through nanopore formation and the production of reactive oxygen species (ROS) (Grandinetti and Reineke, 2012; Grandinetti et al., 2012). Moreover, the toxicity of PAMAM and other polycationic vectors have been shown to be directly related to the concentration of free polymer (Duncan and Izzo, 2005; Jevprasesphant et al., 2003; Lv et al., 2006; Malik et al., 2000). More recently, Grandinetti et al. (Grandinetti et al., 2012) proved that the potent cationic carriers such as polyethylenimine (PEI) can induce a high amount of plasma membrane and nuclear envelope nanopore formation and they expected that the more toxicity of carrier is related to its bigger size and net positive charge amount. In their report, they noticed that ROS hypothesis had a negligible role on cytotoxicity. It has been confirmed that PAMAM has similar effect on biological membranes as PEI in nanopore formation (Lee and Larson, 2008; Mecke et al., 2005), thus it seems that the same as PEI, more cytotoxicity could also result from the polyplexes formed at the higher charge ratios for PAMAM. However, to yield insight into the exact mechanism of PAMAM cytotoxicity, more studies are needed.

Prior to investigate the nuclear uptake kinetics, cellular uptake experiments implied that for both PAMAM and Lipofectamine™, GAGs- and HSPG-deficient cells had collectively a higher internalization than CHO parent cells (Fig. 4A). This means that the new approaches which the mutant cells used to compensate the absence of GAGs- or HSPG-mediated route of internalization are more efficient mechanisms than GAGs-dependent pathway. Our previous observation (Ruponen et al., 2001) indicates that beside GAGs, there are other negatively charged molecules on the cell surface which can promote cellular uptake of the complexes in the absence of GAGs. The nature of these molecules and GAGs-free mechanisms of cellular internalization would be interesting to be clarified.

At the nuclear delivery step, regarding the kinetic aspects of the transfection, PAMAM delivers pDNA to the nucleus at a similar rate

to the other reported non-viral vectors (Hama et al., 2007; Hama et al., 2006; Tachibana et al., 2002; Varga et al., 2005). The present study indicates that the pDNA reaches its maximum concentration (C_{max}) at around 8 h post-transfection with PAMAM–pDNA complexes. The fastest elimination rate was in case of HSPG-deficient cells. CHO parent cells showed the lowest rate of pDNA elimination (Table 2).

Besides the rate and amount, the half-life of delivered pDNA and expressed protein is of importance in kinetics, too. The half-lives of luciferase activity were reported to be 16 and 48 h with Lipofectamine plus™ transfection in NIH3T3 and HeLa cells, respectively (Yamada et al., 2005). Except for GAGs-deficient cells, the half-lives of luciferase intensity in the present research were found to be lower than 12 h for two other cell lines (CHO and HSPG-deficient cells). Many probable reasons could interfere in the final half-lives of expression (Hama et al., 2007). For example, this observed shorter half-life could be due to the interferences in the transcription or translation process caused by the GAGs-dependent uptake pathway. However, to make a clear decision on this topic more detailed evaluations are necessary.

In a report 5% of the administered pDNA dose reached the nucleus using Lipofectamine™ in both NIH3T3 and HeLa cells(Yamada et al., 2005). Our findings indicate that PAMAM were 8-fold more efficient in nuclear delivery, based only upon total GAGs elimination than CHO parent cells (Fig. 5A). HSPG-eliminated cells were as efficient as CHO parent cells in nuclear delivery. This finding was also consistent to the results of cellular uptake, wherein higher internalization had been observed in the absence of GAGs, whereas HSPG-negative cells had the cellular uptake rather lower than GAGs-free cells.

This study shows that in general, total absence of GAGs increased cellular and nuclear uptake of the PAMAM–pDNA complexes by nearly three and eight folds, respectively and resulted in more than 2.6-fold higher transfection efficiency. The results of transfection efficiency are in good agreement with prior observations by us (Lampela et al., 2004; Ruponen et al., 2004) and some other researchers (Belting and Petersson, 1999).

In addition to the cellular uptake results, further study at nuclear and protein expression steps confirmed that neither AUC of nuclear uptake, nor AUC of protein expression was affected significantly by only HSPG elimination in comparison with the CHO parent cells. This findings challenge the theory of regarding all the cell-surface HSPG as the promoting primary receptors of polycationic gene delivery and expression (Mislick and Baldeschwieler, 1996). In this theory syndecans (SDC), as a family of cell-surface HSPG, are regarded as the most probable primary receptors of cationic non-viral vector/gene complexes. In a report, the opposite roles have been proposed for even different family members of SDC (Paris et al., 2008). Subfamily of SDC1 had been found to be in favor of both cell uptake of complexes and protein expression. Although SDC2 showed the same cell uptake promoting behavior, but its post-delivery downstream processes were not efficient in protein expression (Paris et al., 2008).

Considering this finding and results of other literatures (Belting and Petersson, 1999; Lampela et al., 2004; Ruponen et al., 2004; Ruponen et al., 2001; Ruponen et al., 1999), it is supposed that GAGs, at least in case of CHO compared with these mutants, have inhibitory mechanisms on the internalization and protein expression. The exact mechanism is not clear, but it could be due to different ratios of SDC family members on the cell surface that can result in different cell uptake amounts and intracellular consequences for gene complexes. The different roles in transfection by the members of SDC family may justify this explanation.

It has been shown that exogenous GAGs can interfere with transcription and translation machineries and processes (Ruponen et al., 2001; 1999). This can occur inside the cells as an inhibitory mechanism of GAGs on transgene expression, since both cell-surface GAGs and gene complexes are present in intracellular uptake and expression pathway (Ruponen et al., 2004).

As mentioned, in GAGs-deficient cells the protein expression increased by 2.6-fold, while the intranuclear pDNA had more than eight folds increase compared with CHO parent cells. This indicates that part of these increased intranuclear pDNA was inefficient in protein production. This inefficiency may arise from defects in mRNA transcription and/or protein translation enzymes and machineries. Indeed, one explanation for this may be that the high amount of intranuclear pDNA in GAG-deficient cells may have saturated the transcription/translation processes.

Additionally, it is obvious that pDNA should be as released or relaxed form prior to be transcribed by the enzymes. Due to the polyanionic nature of GAGs, they can interact more efficiently than free ions to replace and relax the pDNA from cationic carrier-pDNA complexes. It has been confirmed that GAGs are able to effectively dissociate the complexes in vitro and in vivo (McLendon et al., 2010). Therefore, presence of GAGs along with the internalized complexes inside the cells, although was shown to decrease the uptake, would facilitate the relaxation and release process of pDNA from complexes. Thus, pDNA release decreases in consequence of lacking GAGs in GAGs-deficient cells and causes deficiency in transcription or translation.

Hama et al. (2007) suggested that there are special zones inside the nucleus matrix called euchromatin zones which are rich in enzymes and therefore are more active in transcription compared with the other regions. Increased GAGs-independent delivery in GAGs-deficient cells would direct part of the delivered pDNA to the regions other than euchromatin regions (called heterochromatin regions) which are inefficient in transcription.

Whether releasing of pDNA, enzymatic deficiency, different delivery pathway for GAGs-deficient cells (heterochromatin zone) or other probable obstacles plays the main role at transgene expression inefficiency in this regard, is another remained question which needs to be clarified. However, the overall increase of transfection in the absence of GAGs dominates the decreased transgene expression efficiency related to the probable mentioned obstacles in consequence of GAGs lacking.

5. Conclusion

In this study, PAMAM G5 was evaluated as a non-viral vector for delivery of pDNA. Physicochemical properties such as size, zeta potential and morphology of the prepared PAMAM–pDNA complexes were suitable for delivery as it was confirmed by fluorescent microscopy, flow cytometry and cytotoxicity assays. Collectively, intracellular kinetics of the complexes revealed that PAMAM suffers from the same problems of post-delivery steps (such as transcription or translation steps) as for other polyfection reagents (Hama et al., 2007; Varga et al., 2005). This means that the main rate-limiting step of PAMAM transfection is after delivery to the cell nucleus.

Moreover, GAGs revealed to be an inhibitory factor for the cell internalization and intranuclear delivery of PAMAM–pDNA in CHO cells, while a slightly promoting factor for the transcription or translation processes.

To our knowledge, this is the first report of intracellular and especially nuclear uptake kinetics of PAMAM–pDNA complexes in relation to the cell-surface GAGs.

Also, this study demonstrated a stronger correlation between cell-surface GAGs elimination and intranuclear delivered pDNA with protein expression by a vector, for the first time.

References

Belting, M., Petersson, P., 1999. Protective role for proteoglycans against cationic lipid cytotoxicity allowing optimal transfection efficiency in vitro. Biochem. J. 342 (Pt 2), 281–286.

Bielinska, A.U., Chen, C., Johnson, J., Baker, J.R., 1999. DNA complexing with polyamidoamine dendrimers: implications for transfection. Bioconjugate Chem. 10, 843–850.

Boulaiz, H., Marchal, J.A., Prados, J., Melguizo, C., Aranega, A., 2005. Non-viral and viral vectors for gene therapy. Cell. Mol. Biol. 51, 3–22.

Bradford, M.M., 1976. A rapid and sensitive method for the quantitation of microgram quantities of protein utilizing the principle of protein-dye binding. Anal. Biochem. 72, 248–254.

Cohen, R.N., van der Aa, M.A., Macaraeg, N., Lee, A.P., Szoka Jr., F.C., 2009. Quantification of plasmid DNA copies in the nucleus after lipoplex and polyplex transfection. J. Control. Release 135, 166–174.

de Assis, D.N., Mosqueira, V.C.F., Vilela, J.M.C., Andrade, M.S., Cardoso, V.N., 2008. Release profiles and morphological characterization by atomic force microscopy and photon correlation spectroscopy of 99m technetium-fluconazole nanocapsules. Int. J. Pharm. 349, 152–160.

Duncan, R., Izzo, L., 2005. Dendrimer biocompatibility and toxicity. Adv. Drug Deliv. Rev. 57, 2215–2237.

Eichman, J.D., Bielinska, A.U., Kukowska-Latallo, J.F., Baker, J., 2000. The use of PAMAM dendrimers in the efficient transfer of genetic material into cells. Pharm. Sci. Technol. Today 3, 232–245.

Grandinetti, G., Reineke, T.M., 2012. Exploring the mechanism of plasmid DNA nuclear internalization with polymer-based vehicles. Mol. Pharm. 9, 2256–2267.

Grandinetti, G., Smith, A.E., Reineke, T.M., 2012. Membrane and nuclear permeabilization by polymeric pDNA vehicles: efficient method for gene delivery or mechanism of cytotoxicity? Mol. Pharm. 9, 523–538.

Haensler, J., Szoka Jr., F.C., 1993. Polyamidoamine cascade polymers mediate efficient transfection of cells in culture. Bioconjugate Chem. 4, 372–379.

Hama, S., Akita, H., Iida, S., Mizuguchi, H., Harashima, H., 2007. Quantitative and mechanism-based investigation of post-nuclear delivery events between adenovirus and lipoplex. Nucleic Acids Res. 35, 1533–1543.

Hama, S., Akita, H., Ito, R., Mizuguchi, H., Hayakawa, T., Harashima, H., 2006. Quantitative comparison of intracellular trafficking and nuclear transcription between adenoviral and lipoplex systems. Mol. Ther. 13, 786–794.

Huang, R.Q., Qu, Y.H., Ke, W.L., Zhu, J.H., Pei, Y.Y., Jiang, C., 2007. Efficient gene delivery targeted to the brain using a transferrin-conjugated polyethyleneglycol-modified polyamidoamine dendrimer. FASEB J. 21, 1117–1125.

Jevprasesphant, R., Penny, J., Jalal, R., Attwood, D., McKeown, N.B., D'Emanuele, A., 2003. The influence of surface modification on the cytotoxicity of PAMAM dendrimers. Int. J. Pharm. 252, 263–266.

Kolhatkar, R.B., Kitchens, K.M., Swaan, P.W., Ghandehari, H., 2007. Surface acetylation of polyamidoamine (PAMAM) dendrimers decreases cytotoxicity while maintaining membrane permeability. Bioconjugate Chem. 18, 2054–2060.

Kukowska-Latallo, J.F., Bielinska, A.U., Johnson, J., Spindler, R., Tomalia, D.A., Baker, J.R., 1996. Efficient transfer of genetic material into mammalian cells using starburst polyamidoamine dendrimers. Proc. Natl. Acad. Sci. USA 93, 4897–4902.

Lampela, P., Soininen, P., Puttonen, K.A., Ruponen, M., Urtti, A., Mannisto, P.T., Raasmaja, A., 2004. Effect of cell-surface glycosaminoglycans on cationic carrier combined with low-MW PEI-mediated gene transfection. Int. J. Pharm. 284, 43–52.

Lee, H., Larson, R.G., 2008. Lipid bilayer curvature and pore formation induced by charged linear polymers and dendrimers: the effect of molecular shape. J. Phys. Chem. B 112, 12279–12285.

Liu, J., Thorp, S.C., 2002. Cell surface heparan sulfate and its roles in assisting viral infections. Med. Res. Rev. 22, 1–25.

Lv, H., Zhang, S., Wang, B., Cui, S., Yan, J., 2006. Toxicity of cationic lipids and cationic polymers in gene delivery. J. Control. Release 114, 100–109.

Malik, N., Wiwattanapatapee, R., Klopsch, R., Lorenz, K., Frey, H., Weener, J.W., Meijer, E.W., Paulus, W., Duncan, R., 2000. Dendrimers: relationship between structure and biocompatibility in vitro, and preliminary studies on the biodistribution of 125I-labelled polyamidoamine dendrimers in vivo. J. Control. Release 65, 133–148.

McLendon, P.M., Buckwalter, D.J., Davis, E.M., Reineke, T.M., 2010. Interaction of poly(glycoamidoamine) DNA delivery vehicles with cell-surface glycosaminoglycans leads to polyplex internalization in a manner not solely dependent on charge. Mol. Pharm. 7, 1757–1768.

Mecke, A., Majoros, I.J., Patri, A.K., James, R., Banaszak Holl, M.M., Orr, B.G., 2005. Lipid bilayer disruption by polycationic polymers: the roles of size and chemical functional group. Langmuir 21, 10348–10354.

Mislick, K.A., Baldeschwieler, J.D., 1996. Evidence for the role of proteoglycans in cation-mediated gene transfer. Proc. Natl. Acad. Sci. USA 93, 12349–12354.

Mitra, A., Imae, T., 2004. Nanogel formation consisting of DNA and poly(amido amine) dendrimer studied by static light scattering and atomic force microscopy. Biomacromolecules 5, 69–73.

Mounkes, L.C., Zhong, W., Cipres-Palacin, G., Heath, T.D., Debs, R.J., 1998. Proteoglycans mediate cationic liposome-DNA complex-based gene delivery in vitro and in vivo. J. Biol. Chem. 273, 26164–26170.

Navarro, G., Tros de ILarduya, C., 2009. Activated and non-activated PAMAM dendrimers for gene delivery in vitro and in vivo. Nanomed. Nanotech. Biol. Med. 5, 287–297.

Nomani, A., Haririan, I., Rahimnia, R., Fouladdel, S., Gazori, T., Dinarvand, R., Omidi, Y., Azizi, E., 2010. Physicochemical and biological properties of self-assembled antisense/poly(amidoamine) dendrimer nanoparticles: the effect of dendrimer generation and charge ratio. Int. J. Nanomed. 5, 359–369.

Paris, S., Burlacu, A., Durocher, Y., 2008. Opposing roles of syndecan-1 and syndecan-2 in polyethyleneimine-mediated gene delivery. J. Biol. Chem. 283, 7697–7704.

Payne, C.K., Jones, A.S., Chen, C., Zhuang, X., 2007. Internalization and trafficking of cell surface proteoglycans and proteoglycan-binding ligands. Traffic 8, 389–401.

Ruoslahti, E., 1988. Structure and biology of proteoglycans. Annu. Rev. Cell Dev. Biol. 4, 229–255.

Ruponen, M., Arkko, S., Urtti, A., Reinisalo, M., Ranta, V.P., 2009. Intracellular DNA release and elimination correlate poorly with transgene expression after non-viral transfection. J. Control. Release 136, 226–231.

Ruponen, M., Honkakoski, P., Tammi, M., Urtti, A., 2004. Cell-surface glycosaminoglycans inhibit cation-mediated gene transfer. J. Gene Med. 6, 405–414.

Ruponen, M., Ronkko, S., Honkakoski, P., Pelkonen, J., Tammi, M., Urtti, A., 2001. Extracellular glycosaminoglycans modify cellular trafficking of lipoplexes and polyplexes. J. Biol. Chem. 276, 33875–33880.

Ruponen, M., Yla-Herttuala, S., Urtti, A., 1999. Interactions of polymeric and liposomal gene delivery systems with extracellular glycosaminoglycans: physicochemical and transfection studies. Biochim. Biophys. Acta – Biomembr. 1415, 331–341.

Singh, S.K., Prasad Verma, P.R., Razdan, B., 2011. Atomic force microscopy, transmission electron microscopy, and photon correlation spectroscopy: three techniques for rapid characterization of optimized self-nanoemulsiying drug delivery system of glibenclamide, carvedilol, and lovastatin. J. Disper. Sci. Technol. 32, 538–545.

Su, C.J., Chen, H.L., Wei, M.C., Peng, S.F., Sung, H.W., Ivanov, V.A., 2009. Columnar mesophases of the complexes of DNA with low-generation poly(amido amine) dendrimers. Biomacromolecules 10, 773–783.

Tachibana, R., Harashima, H., Ide, N., Ukitsu, S., Ohta, Y., Suzuki, N., Kikuchi, H., Shinohara, Y., Kiwada, H., 2002. Quantitative analysis of correlation between number of nuclear plasmids and gene expression activity after transfection with cationic liposomes. Pharm. Res. 19, 377–381.

Tang, M.X., Redemann, C.T., Szoka, F.C., 1996. In vitro gene delivery by degraded polyamidoamine dendrimers. Bioconjugate Chem. 7, 703–714.

Tomalia, D.A., Baker, H., Dewald, J., Hall, M., Kallos, G., Martin, S., Roeck, J., Ryder, J., Smith, P., 1984. New class of polymers: starburst dendritic macromolecules. Polym. J. 17, 117–132.

Tuve, S., Wang, H., Jacobs, J.D., Yumul, R.C., Smith, D.F., Lieber, A., 2008. Role of cellular heparan sulfate proteoglycans in infection of human adenovirus serotype 3 and 35. PLoS Pathog. 4, e1000189.

Varga, C.M., Tedford, N.C., Thomas, M., Klibanov, A.M., Griffith, L.G., Lauffenburger, D.A., 2005. Quantitative comparison of polyethylenimine formulations and adenoviral vectors in terms of intracellular gene delivery processes. Gene Ther. 12, 1023–1032.

Wang, W., Xiong, W., Wan, J., Sun, X., Xu, H., Yang, X., 2009. The decrease of PAMAM dendrimer-induced cytotoxicity by PEGylation via attenuation of oxidative stress. Nanotechnology 20, 105103.

Yamada, Y., Kamiya, H., Harashima, H., 2005. Kinetic analysis of protein production after DNA transfection. Int. J. Pharm. 299, 34–40.

Yang, S., May, S., 2008. Release of cationic polymer–DNA complexes from the endosome: a theoretical investigation of the proton sponge hypothesis. J. Chem. Phys. 129, 185105.